Neuron
Article

A Map for Horizontal Disparity in Monkey V2

Gang Chen,[1] Haidong D. Lu,[1] and Anna W. Roe[1,*]
[1]Department of Psychology, Vanderbilt University, Nashville, TN 37203, USA
*Correspondence: anna.roe@vanderbilt.edu
DOI 10.1016/j.neuron.2008.02.032

SUMMARY

The perception of visual depth is determined by integration of spatial disparities of inputs from the two eyes. Single cells in visual cortex of monkeys are known to respond to specific binocular disparities; however, little is known about their functional organization. We now show, using intrinsic signal optical imaging and single-unit physiology, that, in the thick stripe compartments of the second visual area (V2), there is a clustered organization of Near cells and Far cells, and moreover, there are topographic maps for Near to Far disparities within V2. Our findings suggest that maps for visual disparity are calculated in V2, and demonstrate parallels in functional organization between the thin, pale, and thick stripes of V2.

INTRODUCTION

Binocular inputs are used by the human visual system to judge object depth in the 3D world. Stimuli nearer or farther from the fixation point will produce disparities from left and right eye with a negative or positive horizontal shift, respectively. Neurons selective for horizontal disparities are first observed in primary visual cortex (V1) and have been characterized with different methodologies. These include response to offset bars presented to the two eyes (“tuned excitatory,” “tuned inhibitory,” “near,” and “far” cells; Poggio and Fischer, 1977), response to differential phase of sinusoidal gratings (Ohzawa and Freeman, 1986), and response to absolute disparity of random dot stereograms (RDSs) (Cumming and Parker, 1997). In the second visual cortex (V2), disparity-selective neurons have been described as “obligatory binocular” (Hubel and Wiesel, 1970), selective for disparity-defined contours (Bakin et al., 2000; Qiu and von der Heydt, 2005), and tuned for relative disparity (Thomas et al., 2002). Despite the number of studies on disparity responses in the visual cortex, there are no published studies addressing any systematic representation of disparity response in either V1 or V2 (Cumming and DeAngelis, 2001).

Of the three featural maps represented in V2, two have been shown to exhibit a topographic organization. Functional maps of contour orientation exhibit systematic orientation structure characterized by pinwheels in the thick and pale stripes (Malach et al., 1994; Ramsden et al., 2001; Xu et al., 2004a). In the thin stripes, color representation in V2 exhibits a systematic topography for hue representation (Xiao et al., 2003) as well as an organization for brightness increment (ON) versus decrement (OFF) representation (Roe et al., 2005b; Wang et al., 2006). Given the known organizations of the other featural maps in V2 (color and contour in the thin and pale/thick stripes of V2, respectively), this gap in our knowledge regarding disparity representation in V2 is particularly conspicuous. Disparity-selective responses are believed to be preferentially localized to the cytochrome oxidase thick stripes of V2, but topographic representation within these stripes has not been examined (Bakin et al., 2000; G.R. Burkitt, J. Lee, and D.Y. Ts’o, personal communication; Hubel and Livingstone, 1987; Peterhans and von der Heydt, 1993; Roe and Ts’o, 1995).

Thus, at issue are the questions of whether there is a map for Near to Far depth information and whether disparity and orientation information, which are both represented in the thick stripes, are independently represented or not. The broader issue of parallelism and modularity across featural domains in V2 is also in question. Examination of these issues is further motivated by the presence of maps organized for disparity in area MT (DeAngelis and Newsome, 1999), a primary target of V2 thick stripes.

RESULTS

To address these questions, we used intrinsic signal optical imaging methodology (Grinvald et al., 1986) and single-unit electrophysiology. Nine hemispheres from six anesthetized monkeys were studied. Eyes were stabilized and prisms were used to position the view of each eye on a monitor. Spot imaging and electrophysiological methods were used to determine the visual extent of the imaging field of view and the precise convergence of the two eyes (Figures S1 and S2, available online). Disparity stimuli consisted of RDSs (random dot textures presented with a relative shift of the dots in one eye relative to the other; Julesz, 1971) presented at different ocular offsets. These stimuli have the advantage of inducing strong percepts of depth (Near or Far depending on the shift between the two eyes) purely by interocular offset, without any dependence on contour orientation, spatial contrast, or spatial frequency, which are complications of both bar and grating stimuli. Such RDSs were presented with 7 or 13 different horizontal disparities to induce percepts of surfaces at depthes ranging from 0.85° near to 0.85° far (see Experimental Procedures). Because the extent of the perceived square (6° × 6°) induced by the RDS was outside the imaged field of view, the imaged signal can be attributed to RDS-induced depth uncontaminated by possible depth-related illusory contour signals (Qiu and von der Heydt, 2005). Uncorrelated stereograms, which contain similar monocular cues as RDSs, failed to induce constant depth surface percepts and were used as control comparisons (Gonzalez and Perez, 1998).

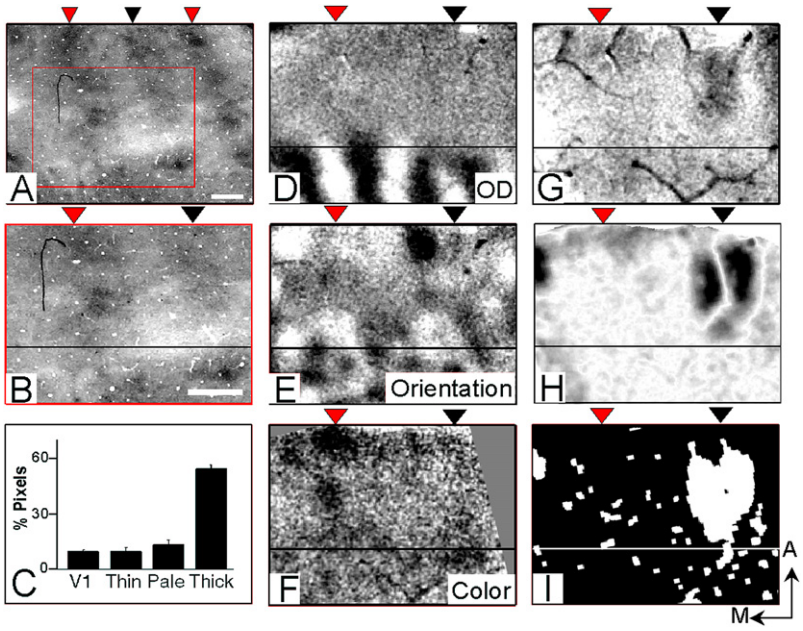

Figure 1. Localization of the Disparity Response in the Thick Stripes of V2

(A) A section stained for cytochrome oxidase showing the positions of thin (red arrow heads) and thick (a black arrow head) stripes of V2.

(B) Enlarged inset of red boxed region in (A).

(C) Percentage of pixels in V1 and in the thin, pale, and thick stripes of V2 with significant ($p < 0.05$) response to RDSs. More pixels in thick stripes ($n = 5$) responded to depth stimuli than those in V1 in the pale or thin stripes within V2 or ($p < 10^{-6}$, Student's t test). Error bars = SEM.

(D) Ocular dominance map in V1 (left eye minus right eye) reveals V1/V2 border (horizontal line).

(E) Orientation map (differential response, horizontal versus vertical gratings).

(F) Thin stripes are determined by the areas that prefer color to luminance. Note that regions with color preference (thin stripes) have poor orientation preference. The gray region is out of field of view because the camera was moved to a slightly different location for the color run.

(G) The difference between binocular stimuli (dark pixels) and monocular stimuli (light pixels) reveals the position of the thick stripe (cf. Ts'o et al., 2001).

(H) RDS disparity map. Sum of all Near and Far.

(I) White pixels are those with significant responses to RDS (compared with responses to uncorrelated stereograms; Student's t test, $p < 0.05$).

Scale bars: (A) and (B), 1 mm. Scale bar for (B) applies to (D)–(I). A, anterior; M, medial.

Preferential Activation in V2 Thick Stripes

Using standard optical imaging techniques, we mapped the locations of the V1/V2 border (Figure 1D), and the thin, pale, and thick stripes in V2 (Blasdel, 1992; Roe et al., 2005a; Ts'o et al., 1990; Xu et al., 2004a). As confirmed with cytochrome oxidase histology (Figures 1A and 1B) and consistent with previous studies, orientation domains overlay thick and pale stripes (Figure 1E), domains for color versus luminance preference overlay thin stripes (Figure 1F), and domains for binocularity versus monocularity overlay thick stripes (Figure 1G).

We found that the areas with significant responses to RDS (based on pixel-by-pixel t test of RDS and uncorrelated stereograms, $p < 0.05$) were preferentially located in the thick stripes of V2 (Figures 1H and 1I). On average, roughly half of the pixels (43.1% ± 3.8%) within thick stripes ($n = 9$) were significantly responsive to at least one of the RDS-defined surfaces (Figure 1C). In comparison, a much lower fraction of the pixels in V1 (8.2% ± 1.2%, $n = 9$), V2 thin stripes (10.6% ± 1.3%, $n = 9$), and V2 pale stripes (14.5% ± 1.5%, $n = 9$) exhibited significant activation to RDSs (Figure 1C). These data suggest a preferential response to RDSs in V2 thick stripes that is not present elsewhere in V2 or in V1. In sum, disparity-selective cells in V2 thick stripes exhibit preferential binocular versus monocular response (Ts'o et al., 2001), responsiveness to depth contours (Bakin et al., 2000; Qiu and von der Heydt, 2005), and responsiveness to surface depth induced by RDS (Thomas et al., 2002). Such organized responses are notably absent from the other stripes of V2 and from V1.

A Map for Horizontal Disparity in V2

To examine possible segregation of Near and Far responses in the thick stripes, we computed a Near minus Far difference map (Figure 2A, obtained by taking the difference of the sums of the three Near conditions and the three Far conditions). In both thick stripes visible in this field of view, this map reveals a clear segregation of Near preference (dark pixels) and Far preference (light pixels). Interestingly, the mediolateral position of Near versus Far appears to differ in these two stripes.

Further examination of single-condition maps revealed a clear Near-to-Far topography. Figures 2B–2H illustrate single-condition maps of one thick stripe (indicated by the dotted box in Figure 2A) in response to each of seven RDS disparity stimuli: Near: 0.34°, 0.17°, and 0.085° (Figures 2B–2D); Zero (Figure 2E); and Far: 0.085°, 0.17°, and 0.34° (Figures 2F–2H). In each panel, the region significantly activated by the RDS stimulus ($p < 0.05$, Student's t test) is outlined in color and appears as an elongated band, roughly 200 μm in width and 1 mm in length. As the stimulus disparity shifts from Near to Far (Figures 2B–2H), the activation band shifts from left to right (medial to lateral). This topography is summarized in Figure 2I (three representative disparities: −0.34° red, 0° green, and +0.34° blue). In comparison, responses to uncorrelated RDSs failed to produce any structured responses (Figure 2J).

A second case is shown in Figure 3. In this case, RDSs elicited multiple foci of activation within a single thick stripe. As horizontal disparity shifted from −0.34°, −0.17°, −0.085°, 0, +0.085°, +0.17°, and +0.34° (Figures 3B–3H, respectively), the location of each of these domains also shifted. If one follows a single activation site (labeled 1, 2, and 3 in Figure 3B), a consistent topography for each site is still evident (shifting outlines shown in Figures 3I–3K). Three more cases are shown in supplementary materials (Figure S3), which include two cases (Case 2 and Case 3) examining a larger disparity range from +0.85° Far to −0.85° Near.

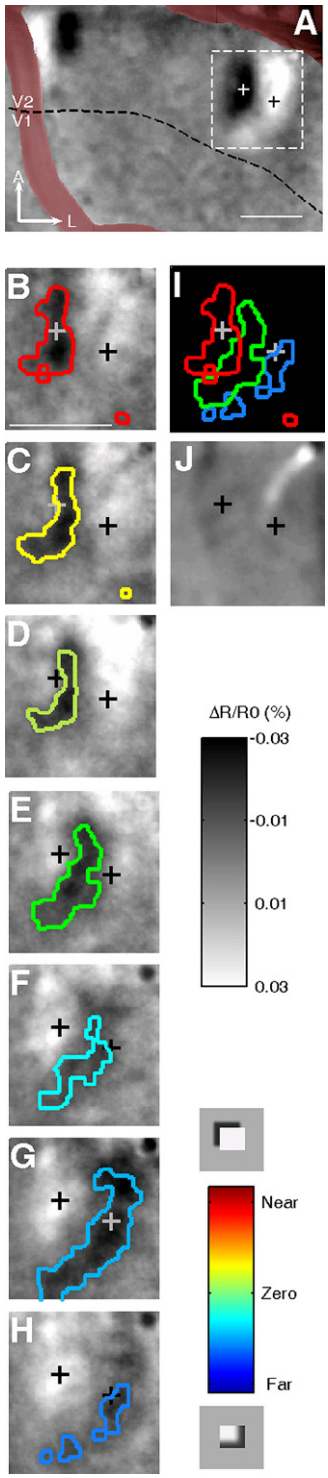

Figure 2. Disparity Topography in V2

(A) Differential image between all Near (dark pixels) and all Far (light pixels) stimuli. Black dashed line, border of V1/V2. (B–H). Single-condition images evoked by three Near stimuli with disparities of 0.34° (B), 0.17° (C), and 0.085° (D); Zero (E); and three Far stimuli of 0.085° (F), 0.17° (G), and 0.34° (H). The positions of the two crosses are constant through (A)–(J). The outlined regions in (B)–(H) show areas with significantly greater response to RDS than to uncorrelated stereograms ($p < 0.05$, Student's t test). As described by ellipse fits, the lengths of these domains in (B)–(H) are 802, 831, 856, 933, 1216, 690, and 918 μm, respectively. Widths are 431, 428, 350, 437, 370, 549, and 298 μm, respectively. (I) Summary showing overlay of three disparity contours (red: 0.34° near; green: zero; blue: 0.34° far). (J) Optical image of response to uncorrelated random dots (versus Blank; a streak of white activity [upper right corner] is due to blood vessel noise). Grayscale: magnitude of imaged response in percent reflectance. Color scale: near to far disparity. Scale bars: (A) and (B), 1 mm. A, anterior; L, lateral.

To quantify this shift, we defined two indices, one to reflect percentage overlap and another to reflect the distance between the centers of different domains (see Experimental Procedures). If representations of disparity in V2 were topographic, then one would predict that domains representing similar disparities would be closer together and exhibit more overlap, while those representing different disparities would be further apart and exhibit less overlap. Figures 4A and 4B support these predictions. As shown in Figure 4A, the overlap ranged from more than 50% for the smallest disparity differences (Δ0.085°, 52.5% ± 2.8%, n = 140) to almost no overlap at disparity differences of more than half a degree (Δ0.68°, 0.2% ± 0.2%, n = 30; Δ0.60°, Δ0.77°, Δ0.85°, Δ0.94°, and Δ1.02°, no overlap). Delta disparity correlates significantly with overlap ($p < 10^{-10}$, ANOVA; correlation regression, $r = 0.42$, $p < 0.01$, $n = 708$); on average, a 1° disparity shift results in a 77.9% decrease in overlap. Similarly, the distance between domains (center of mass) varied with delta disparity ($p < 10^{-10}$, ANOVA; Figure 4B). Over the disparity range tested, the distance between centers increased from 180 μm (Δ0.085°, 181.6 ± 21.5 μm, n = 70) to almost four times greater (Δ0.65°, 699.6 ± 153.4 μm, n = 4) with increasing disparity. These tendencies were found in all six animals we tested (Figure S4).

Cortical magnification is an important aspect of any topographic map. The possibility that there exist differential cortical magnifications across a parameter space can indicate the relative importance or precision of that parameter within certain ranges of that space. We therefore considered the possibility that magnifications are greater or smaller within the range of depths examined. However, when the size and shape of the activated bands were measured by fitting the iso-disparity regions with ellipses (Figures 4C–4E), we found that on average the length and width of Near domains (red, n = 45), Zero domains (green, n = 50), and Far domains (blue, n = 28), did not differ from each other (both $p > 0.5$, ANOVA). Based on this roughly even representation within the −0.5° to +0.5° disparity and the measurements in Figures 4A and 4B, the cortical magnification factor of disparities is on average 1° per 780 μm.

Neural Basis

To examine the neuronal basis of the optical signal, we targeted imaged disparity domains with microelectrodes and recorded single-unit activity from the superficial cortical layers (Figure 5A; same field view as Figures 2B–2J). In each penetration, one to four units were isolated and disparity tuning curves were obtained. Within each penetration, cells shared similar tuning preferences (Figure 5B), consistent with previous recordings within vertical penetrations (Ts'o et al., 2001). We then normalized and averaged disparity tuning curves recorded in each

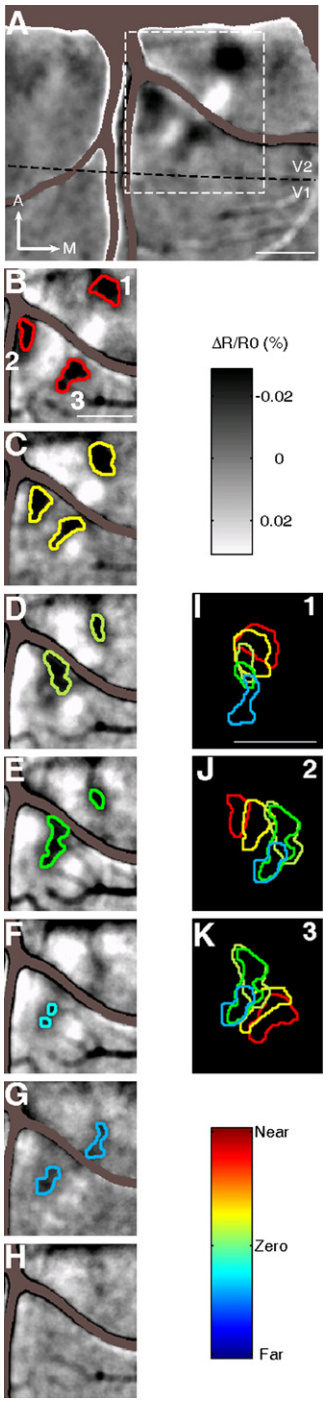

Figure 3. Disparity Topography in V2: A Second Case

(A) Differential image between all Near (dark pixels) and all Far (light pixels) stimuli. Dotted box: region shown in (B)–(K). Black dashed line: V1/V2 border. (B–H) Single-condition disparity images: −0.34° (B), −0.17° (C), −0.085° (D), zero (E), +0.085° (F), +0.17° (G), and +0.34° (H). Three activation domains are labeled 1, 2, and 3 in (B). Color outlines: regions of significant activation ($p < 0.05$, Student's t test). (I-K) Summary topographies of domains 1 (I), 2 (J), and 3 (K). Conventions are the same as in Figure 2. Scale bars: 1 mm. A, anterior; M, medial.

penetration. Plotted in Figure 5D is the average neuronal disparity tuning curve for each of the four penetrations shown in Figure 5A. We then compared this neural tuning curve to the optical responses at each recording location (Figure 5C). Comparison of Figures 5C and 5D reveal that the neuronal and optical response at these four locations had similar tuning curves (Figure 5E; robust fit, $r = 0.80$, $p < 0.01$, $n = 28$). In fact, for the entire population of responses we recorded (individual tuning curves are shown in Figure S5), the average neuronal disparity response preference showed significant correlation with optical disparity response preference (Figure 5F, robust fit, $r = 0.84$, $p < 0.01$, $n = 27$). A similar tendency was found for disparity tuning width (Figure 5G; robust fit, $r = 0.73$, $p < 0.01$, $n = 27$). Deviations from a perfect correlation and tuning width extracted from optical signal can be at least partly attributed to the fact that the optical signal derives from a population average of neuronal responses. Thus, the neuronal responses are consistent with the presence of topography for disparity in V2 and indicate the presence of neurons that respond to RDSs.

Relationship to Orientation

A central issue in cortical representation is how multiple maps coexist within the same 2D cortical space. In V1, many modeling studies suggest that competing intracortical influences result in observed functional organizations for ocular dominance and orientation (Swindale, 2004). In V2, studies suggest an interdigitation of different featural maps that parallel the stripe-like organization revealed in cytochrome oxidase stains (Roe and Ts'o, 1995; Swindale, 2004). However, the relative organization of orientation and disparity in V2 has been elusive. Electrophysiological evidence suggests that representation of horizontal disparity might be biased for vertical orientations (Cumming, 2002: the frequency of cells with horizontal orientation preference is about one third of that with vertical orientation preference in V1; Hubel and Wiesel, 1970). This suggests a possible overrepresentation of vertical orientation relative to horizontal orientation within the V2 thick stripes.

To investigate this corepresentation of orientation and disparity within V2, we examined representation of disparity within orientation domains and the representation of orientation within disparity domains. In this analysis, we considered only the pixels that exhibited significant disparity response (Figure 6A). We found that the disparity-activated regions contained roughly equal representation for different orientations (Figure 6B; $p > 0.9$, ANOVA, $n = 9$) and that on average each orientation domain overlaid a range of disparity domains (Figure 6C; no significant influence from disparity alone, orientation alone, or an interaction between disparity and orientation, all $p > 0.8$, balanced two-way ANOVA, $n = 9$). Thus, we found no evidence for increased or biased disparity representation in vertical orientation domains. Furthermore, we tested whether or not the sensitivities to disparity are similar among different orientation domains. We compared the disparity tuning strength within different orientation domains and found that neurons in the horizontal orientation domains are as sharply tuned for disparity as neurons in other orientation domains (Figure 6D; $p > 0.9$, ANOVA, $n = 9$). Our data suggest, at least for the disparity ranges tested here, orthogonality between the disparity and orientation parameters within the V2 thick stripes (Figure 7).

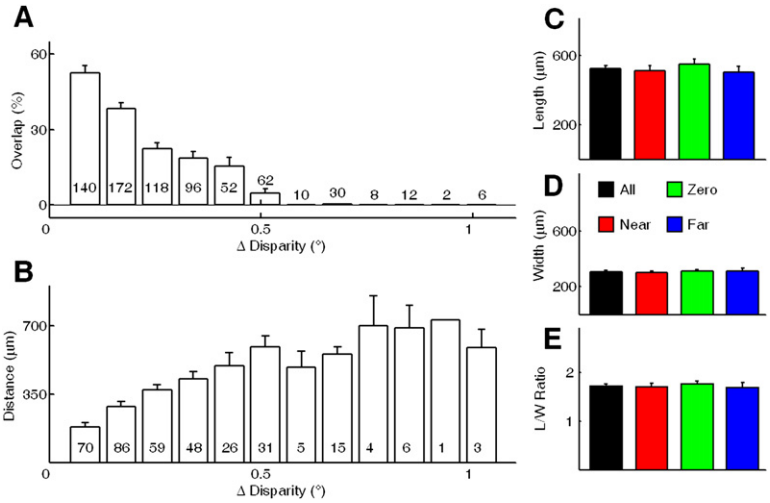

Figure 4. Overlap and Distance Measurements Support Topography

(A) Percent overlap between pairs of disparity domains. Percent overlap predicts delta disparity: the greater the overlap, the more similar the disparity.

(B) Distance between centers of mass of disparity domains. Distance predicts delta disparity: smaller distances predict similar disparity. Numbers of domain pairs are indicated by numbers in bars. Since no two disparity domains have delta disparity larger than 1.1°, the largest bin shown is 1.1° of disparity difference.

(C–E) Average length, width, and length-width ratio of All (black, n = 123), Near (red, n = 45), Zero (green, n = 50), and Far (blue, n = 28) from nine cases. Error bars = SEM.

DISCUSSION

Disparity Response in V2

The role of V2 in depth perception has long been hypothesized. Disparity-selective cells, especially those termed obligatory binocular, are prevalent in V2 (Baizer et al., 1977; Hubel and Wiesel, 1970). The role of V2 in depth perception is further supported by the presence of cells that exhibit response to disparity-defined contours and disparity capture response (Bakin et al., 2000; Qiu and von der Heydt, 2005), to relative over absolute disparity (Thomas et al., 2002), and to stereopsis-choice-related activity (Nienborg and Cumming, 2006, 2007). Functional MRI studies have also found significant disparity-induced activations within V2 (Sereno et al., 2002; Tsao et al., 2003). The preferential, though not exclusive, localization of disparity response to the thick stripes of V2 has been demonstrated electrophysiologically (Bakin et al., 2000; Hubel and Livingstone, 1987; Peterhans and von der Heydt, 1993) and with optical imaging methods that localized preferential response to two eyes over one eye (Ts'o et al., 2001).

Disparity Topography in V2

Although the functional organization of V2 thick stripes was poorly understood, it was suggested that disparity, like color and contour, is represented in a modular fashion (Hubel and Livingstone, 1987; Roe, 2003; Roe and Ts'o, 1995; Ts'o et al., 2001). The possible presence of clustered organization is one indicator of organized topography. Ts'o et al. (2001) reported that the orientation of obligatory binocular cells in vertical penetrations tends to be similar, although they found that disparity tuning shifted slightly with depth, an observation that may be related to slightly off-orthogonal penetrations. Evidence for clustered response in V2 is also reported by Nienborg and Cumming (2006) who found that preferred disparities of multi- and single-unit recordings from the same location were similar. A similar but weaker tendency was found in V1 (Prince et al., 2002). Our small sample of electrophysiological recordings is also consistent with the presence of columnar organization (Figure 5B).

With optical imaging it is possible to observe topographic organizations at the submillimeter scale. In this study, we found that horizontal disparity is mapped in a topographic fashion in V2. Domains were on the order of 200 μm in width and mapped in a systematic fashion within thick stripes. In some cases, multiple topographic disparity maps were observed within V2 thick stripes (Figure 3). It is possible these multiple domains could represent different visuotopic locations in space. Alternatively, different disparity-selective clusters could represent different functionalities that further differentiate different types of disparity response (e.g., those related to motion borders). Such functional distinctions would parallel those found in other stripe types (e.g., hue versus ON/OFF domains within V2 thin stripes). This is an interesting issue that remains to be investigated.

The presence of topographic organization within the thick stripes is consistent with the presence of featural maps for color and contour in thin and pale stripes, respectively. Functional maps of contour orientation, both real contour response and illusory contour response, exhibit systematic orientation structure characterized by pinwheels in the thick and pale stripes (Roe and Ts'o, 1995; Ts'o et al., 2001). In the thin stripes, color representation in V2 exhibits a systematic topography for hue representation (Xiao et al., 2003), as well as an organization for brightness increment versus decrement representation (Wang et al., 2006). Our findings extend this organization to the thick stripes and a consistent framework for understanding V2 function.

Relationship between Disparity and Orientation Response

We found that orientation and horizontal disparity are mapped somewhat independently. Although some studies report a predominance of disparity-selective cells that prefer vertical orientations (Hubel and Wiesel, 1970; Poggio and Fischer, 1977), our study finds no such preferential association. Indeed, disparity-responsive regions contained orientation response for all orientations tested in roughly equal proportions, and orientation domains contained a range of disparity responses. However, the possibility remains that the disparity-selective response evoked by a 6.0° × 6.0° region in depth may stimulate a different population of cells than those responsive to contour disparity.

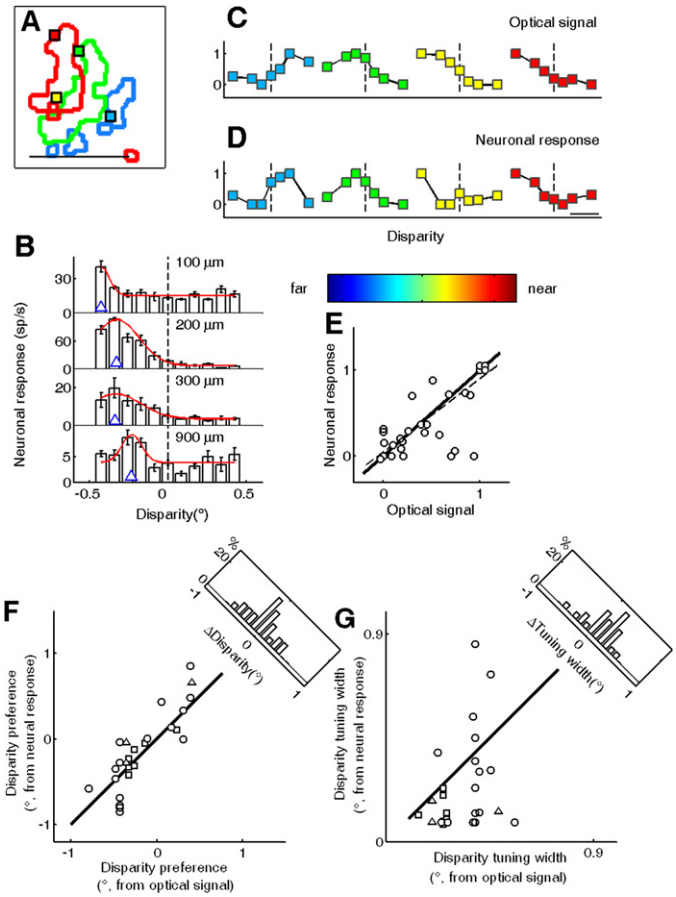

Figure 5. Comparison between Neuronal and Optical Signals

(A) Four electrode-recording locations (marked by colored squares) within the color-coded disparity domains (see color scale bar). (B) Example consistent with columnar organization. Disparity tuning of four neurons recorded within a single vertical penetration is shown. Red lines: Gaussian fit. Blue triangles: preferred disparity. (C and D) Normalized optical (C) and neural (D) disparity tuning curves at each of four locations in (A). Dashed vertical lines indicate zero disparity. (E) Scatter plot for each pair of optical (abscissa) and neuronal (ordinate) signals in (C) and (D), showing significant correlation (robust regression, $r = 0.80$, $p < 0.01$). Scatter plot for disparity preference (F) and disparity tuning width (G) obtained from optical and neuronal signals from three cases is shown ($n = 27$). Disparity preferences are similar ($p > 0.4$, paired t test) while tuning widths tend to be wider than optical signals (see histograms at upper right corners; $p < 0.01$, paired t test). Different marker shapes are neurons recorded from different monkeys. For detailed optical and neuronal tuning curves, see Supplementary materials (Figure S5). Thick lines are diagonals. Scale bars: (A), 1 mm; (D), 0.25°. Error bars = SEM.

Disparity Organizations in Other Areas

Other cortical areas in primate besides V2 also exhibit functional architecture for horizontal disparity. In macaque MT, disparity-tuned neurons are organized in a columnar fashion and, within disparity-preferring regions, exhibit a smoothly shifting topographic organization for disparity selectivity (DeAngelis et al., 1998; DeAngelis and Newsome, 1999). In V3 (Adams and Zeki, 2001) and V4 (Watanabe et al., 2002), neurons with similar disparity selectivity are clustered. Input from V2 might play an important role in either forming or conferring organization in these areas. V3 has major connections with area V2 (Felleman et al., 1997; Stepniewska and Kaas, 1996), and V4 receives inputs both from V2 and from V3 (Stepniewska and Kaas, 1996; Zeki and Shipp, 1989). In particular, because thick stripes of V2, unlike the thin or pale stripes, project directly to MT (DeYoe and Van Essen, 1985; Shipp and Zeki, 1985, 1989), this raises the possibility that the systematic organization of disparity in MT is initiated in V2. This possibility is further strengthened by the finding that inactivation of V2/V3 attenuates the sensitivity of MT neurons to binocular disparity (Ponce et al., 2008). Thus, V2 may be an important bridge both for generalizing depth-related activity from V1 (Bakin et al., 2000; Cumming and Parker, 1999; Thomas et al., 2002) and for conferring organized depth-related information to higher cortical areas.

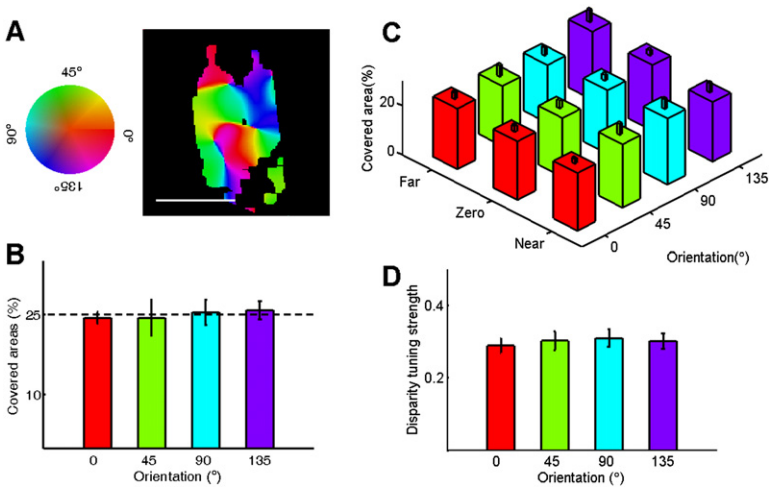

Figure 6. Relationship between Orientation Domains and Disparity Domains

(A) The orientation selectivity of areas with significant response to any disparity tested (same case as shown in Figure 1). The preferred orientations are shown (color wheel). Scale bar: 1 mm.

(B) Percentage of pixels (of the disparity-selective pixels) at each of the 0°, 45°, 90°, and 135° orientations. Within disparity-selective pixels, across all cases, the average percentage of areas covered by each orientation was not significantly different from 25% (all $p > 0.5$, Student's t test).

(C) Statistical results of the average percentage of pixels in an orientation domain covered by different disparity domains. Based on a balanced two-way ANOVA, where the factors were disparity, orientation, and their interaction, there is no significant influence from orientation or from disparity (both $p > 0.8$), or significant influence or between them ($p > 0.9$).

(D) Averaged disparity tuning strength within orientation preference domains. No significant difference was found between horizontal and 45°, 90°, or 135° orientation preference domains (all $p > 0.5$, Student's t test, $n = 9$).

Error bars = SEM.

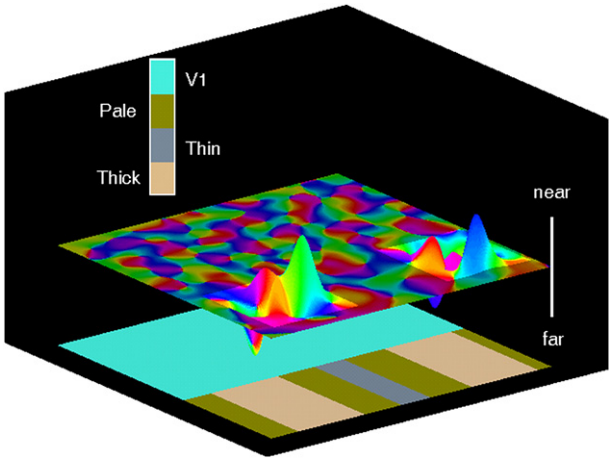

Figure 7. Possible Organization in V2
Depiction of possible organization in V2, where orientation and disparity parameters are orthogonally represented.

In summary, this study demonstrates topography for disparity in V2. Localization of this topography to the thick stripes of V2 further suggests that modular organization is a feature shared across different stripe types and different featural spaces in V2. The additional constraints provided by these data will be useful for models of functional organization within and beyond V1. These data also raise the possibility that at least some aspects of the disparity organizations observed in MT derive from V2 and are not established de novo in MT.

EXPERIMENTAL PROCEDURES

Visual Stimulus and Data Collection

Experiments were preformed under protocols conforming to guidelines of the National Institutes of Health and approved by Vanderbilt University Animal Care and Use Committees. Detailed procedures are described elsewhere (Roe et al., 2005b). Briefly, macaque monkeys were anesthetized (i.v., thiopental sodium, 1–2 $mg \cdot kg^{-1} \cdot h^{-1}$), paralyzed with vercuronium bromide (i.v., 100 $\mu g \cdot kg^{-1} \cdot h^{-1}$), and artificially ventilated. Anesthetic depth was assessed continuously by EEG, end-tidal CO_2, pulse oximetry, and heart rate. Eyes were dilated (atropine sulfate) and fitted with contact lenses to focus on a monitor 76.2 cm from the eyes. Craniotomy and durotomy were performed to expose visual areas V1 and V2.

Visual stimuli were generated with custom software and were presented at 100 Hz. Each eye was stimulated independently, by diverging eyes with Risley prisms to direct them to different parts of the screen. RDSs that produce constant-depth surface percepts (50% dark [0.0 $cd \cdot m^{-2}$]/50% bright [80.0 $cd \cdot m^{-2}$] dots; dot size at 0.085° × 0.085°; dot density at 100%) were presented on a gray background (40.0 $cd \cdot m^{-2}$). A new dot pattern was presented every 100 ms. Horizontal binocular disparities were introduced by shifting the location of dots in the two eyes. The stereograms consisted of an 8.5° × 8.5° square background region maintained at zero disparity, and a 6.0° × 6.0° center patch whose disparity was varied from trial to trial. The tested disparity levels ranged between −0.85° (crossed) and +0.85° (uncrossed). In six hemispheres, we tested seven different disparity levels (three Near: 0.34°, 0.17°, and 0.085°; Zero: 0°; and three Far: 0.085°, 0.17°, and 0.34°) during imaging sessions. Single units were tested from −0.425° to +0.425° with steps of 0.085°. A wider range of disparities were tested on the remaining three hemispheres (13 levels; 6 Near: 0.85°, 0.68°, 0.51°, 0.34°, 0.17°, and 0.085°; Zero: 0°; and six Far: 0.085°, 0.17°, 0.34°, 0.51°, 0.68°, and 0.85°) during imaging sessions, and single units were tested from −0.85° to +0.85° with steps of 0.17°. Uncorrelated stereograms, which do not elicit a constant-depth surface percept, were used as controls. Full-screen square gratings (spatial resolution: 1 cycle/degree) were used to test the orientation preference of the visual cortex.

To eliminate possible ocular drift, eyes were stabilized with eye rings. In addition, eye position was repeatedly checked throughout the experiment by a rapid, high-spatial-precision spot imaging method (Figures S1 and S2). Rapid spot imaging was also used to confirm that the imaged field of view lay well within the bounds of the RDS depth square.

Images of cortical reflectance change (intrinsic signals) were acquired by using IMAGER 3001 (Optical Imaging, Germantown, NY) and 630 nm illumination. For each condition, 30 trials were presented. Areas containing extensive vascular artifact were excluded from analysis.

Data Analysis

In our standard optical imaging analysis, signal-to-noise ratio was enhanced by trial averaging. Images were smoothed by a disc mean filter kernel (radius 80 μm). Low-frequency noise was reduced by convolving the image with an 800 μm radius mean filter kernel and subtracting the result from the original image (Xu et al., 2004b). Single-condition disparity maps (Figure 2 and Figure 3) were obtained by summing frames over 3 s and subtracting control maps. Because, across trials, the pixel response is normally distributed (Lilliefors test, 93.4% ± 0.2% pixels with $p > 0.05$, $n = 12$), we used Student's t test to test the significance. Areas (larger than 100 μm in diameter) were considered to have significant activation ($p < 0.05$) when on average the response of optical signals to the RDS is greater than that to uncorrelated stereogram controls based on a trial-trial comparison. Activation zones were fitted with an ellipse (Fitzgibbon et al., 1999). The following indices were calculated.

Center of mass:

$$[\,COM_x\ COM_y\,] = \left[\frac{1}{n}\sum_{i=1}^{n} x_i \ \frac{1}{n}\sum_{i=1}^{n} y_i\right].$$

Distance between domains:

$$DCOM = \sqrt{(COM_{x,1} - COM_{x,2})^2 + (COM_{y,1} - COM_{y,2})^2}$$

Overlap between domains A and B:

$$POO_{A,B} = \frac{Area_{A\cap B}}{Area_A} \times 100,$$

with $Area_{A\cap B}$ being size of the area common to A and B.

Disparity tuning strength,

$$S = \frac{|R_{max} - R_{min}|}{|R_{max} - R_{min}| + 2 \times \sqrt{\frac{SSE}{N-M}}},$$

was defined in a manner similar to disparity discrimination index (DeAngelis and Uka, 2003; Hinkle and Connor, 2005; Prince et al., 2002), where *SSE* is the sum squared error around the mean responses, *N* is the total number of stimulus presentations, *M* is the number of different disparities tested, and R_{max} and R_{min} represent the mean responses to the most effective and least effective stimuli, respectively. This index lies between 0 and 1. A larger index indicates more sharply tuned disparity.

The color-coded orientation preference map was derived from pixel-by-pixel vector summation (Blasdel, 1992; Bonhoeffer and Grinvald, 1991; Bosking et al., 1997). Two-tailed t test was applied except where indicated.

Electrical Recording

For each recording, two single neurons were isolated, one in V1 (a binocular cell used as a reference cell [Anzai et al., 1999; Ferster, 1981; Hubel and Wiesel, 1970; Roe and Ts'o, 1995]) and one in V2. For each V2 cell isolated, the center of the receptive field was plotted and the RDS was centered on the receptive field of each eye. Different horizontal disparities were presented for 2 s each. A gray screen was presented during the 2 s interstimulus interval. RDS conditions were interlaced in pseudorandom fashion (three to ten repetitions each). Disparity tuning curves were fit with Gaussians by robust regression. For cells with tuned inhibitory tuning curves, negative-going Gaussians were used. For average tuning curves, responses to different disparities were normalized. Error bars are ±SEM.

Histology

At the end of experiments, animals were given a lethal dose of sodium pentothal. Cytochrome-stained tissue was aligned with optical images using lesion sites, cytochrome oxidase landmarks, and blood vessels as guides (Roe et al., 2005a; Shmuel et al., 2005; Xu et al., 2004a).

SUPPLEMENTAL DATA

The Supplemental Data for this article can be found online at http://www.neuron.org/cgi/content/full/58/3/442/DC1/.

ACKNOWLEDGMENTS

We thank Drs. F. Tong and V. Casagrande for suggestions about this manuscript, and Drs. Y. Kamitani and X. Zha for discussion, Peter Kasken for histology, Daniel Shima for programming, Yanyan Chu for technical assistance, and Dr. Jon Kaas for providing eye rings. This work was supported by NIH grant EY 11744 to A.W.R, Vanderbilt Vision Research Center, and Vanderbilt University Center for Integrative & Cognitive Neuroscience.

Received: July 9, 2007
Revised: December 26, 2007
Accepted: February 8, 2008
Published: May 7, 2008

REFERENCES

Adams, D.L., and Zeki, S. (2001). Functional organization of macaque V3 for stereoscopic depth. J. Neurophysiol. *86*, 2195–2203.

Anzai, A., Ohzawa, I., and Freeman, R.D. (1999). Neural mechanisms for encoding binocular disparity: receptive field position versus phase. J. Neurophysiol. *82*, 874–890.

Baizer, J.S., Robinson, D.L., and Dow, B.M. (1977). Visual responses of area 18 neurons in awake, behaving monkey. J. Neurophysiol. *40*, 1024–1037.

Bakin, J.S., Nakayama, K., and Gilbert, C.D. (2000). Visual responses in monkey areas V1 and V2 to three-dimensional surface configurations. J. Neurosci. *20*, 8188–8198.

Blasdel, G.G. (1992). Orientation selectivity, preference, and continuity in monkey striate cortex. J. Neurosci. *12*, 3139–3161.

Bonhoeffer, T., and Grinvald, A. (1991). Iso-orientation domains in cat visual cortex are arranged in pinwheel-like patterns. Nature *353*, 429–431.

Bosking, W.H., Zhang, Y., Schofield, B., and Fitzpatrick, D. (1997). Orientation selectivity and the arrangement of horizontal connections in tree shrew striate cortex. J. Neurosci. *17*, 2112–2127.

Cumming, B.G. (2002). An unexpected specialization for horizontal disparity in primate primary visual cortex. Nature *418*, 633–636.

Cumming, B.G., and Parker, A.J. (1997). Responses of primary visual cortical neurons to binocular disparity without depth perception. Nature *389*, 280–283.

Cumming, B.G., and Parker, A.J. (1999). Binocular neurons in V1 of awake monkeys are selective for absolute, not relative, disparity. J. Neurosci. *19*, 5602–5618.

Cumming, B.G., and DeAngelis, G.C. (2001). The physiology of stereopsis. Annu. Rev. Neurosci. *24*, 203–238.

DeAngelis, G.C., and Newsome, W.T. (1999). Organization of disparity-selective neurons in macaque area MT. J. Neurosci. *19*, 1398–1415.

DeAngelis, G.C., and Uka, T. (2003). Coding of horizontal disparity and velocity by MT neurons in the alert macaque. J. Neurophysiol. *89*, 1094–1111.

DeAngelis, G.C., Cumming, B.G., and Newsome, W.T. (1998). Cortical area MT and the perception of stereoscopic depth. Nature *394*, 677–680.

DeYoe, E.A., and Van Essen, D.C. (1985). Segregation of efferent connections and receptive field properties in visual area V2 of the macaque. Nature *317*, 58–61.

Felleman, D.J., Burkhalter, A., and Van Essen, D.C. (1997). Cortical connections of areas V3 and VP of macaque monkey extrastriate visual cortex. J. Comp. Neurol. *379*, 21–47.

Ferster, D. (1981). A comparison of binocular depth mechanisms in areas 17 and 18 of the cat visual cortex. J. Physiol. *311*, 623–655.

Fitzgibbon, A., Pilu, M., and Fisher, R.B. (1999). Direct Least Square Fitting of Ellipses. IEEE Trans. Pattern Anal. Mach. Intell. *21*, 476–480.

Gonzalez, F., and Perez, R. (1998). Neural mechanisms underlying stereoscopic vision. Prog. Neurobiol. *55*, 191–224.

Grinvald, A., Lieke, E., Frostig, R.D., Gilbert, C.D., and Wiesel, T.N. (1986). Functional architecture of cortex revealed by optical imaging of intrinsic signals. Nature *324*, 361–364.

Hinkle, D.A., and Connor, C.E. (2005). Quantitative characterization of disparity tuning in ventral pathway area V4. J. Neurophysiol. *94*, 2726–2737.

Hubel, D.H., and Wiesel, T.N. (1970). Stereoscopic vision in macaque monkey. Cells sensitive to binocular depth in area 18 of the macaque monkey cortex. Nature *225*, 41–42.

Hubel, D.H., and Livingstone, M.S. (1987). Segregation of form, color, and stereopsis in primate area 18. J. Neurosci. *7*, 3378–3415.

Julesz, B. (1971). Foundations of Cyclopean Perception (Chicago: The University of Chicago Press).

Malach, R., Tootell, R.B., and Malonek, D. (1994). Relationship between orientation domains, cytochrome oxidase stripes, and intrinsic horizontal connections in squirrel monkey area V2. Cereb. Cortex *4*, 151–165.

Nienborg, H., and Cumming, B.G. (2006). Macaque V2 neurons, but not V1 neurons, show choice-related activity. J. Neurosci. *26*, 9567–9578.

Nienborg, H., and Cumming, B.G. (2007). Psychophysically measured task strategy for disparity discrimination is reflected in V2 neurons. Nat. Neurosci. *10*, 1608–1614.

Ohzawa, I., and Freeman, R.D. (1986). The binocular organization of simple cells in the cat's visual cortex. J. Neurophysiol. *56*, 221–242.

Peterhans, E., and von der Heydt, R. (1993). Functional organization of area V2 in the alert macaque. Eur. J. Neurosci. *5*, 509–524.

Poggio, G.F., and Fischer, B. (1977). Binocular interaction and depth sensitivity in striate and prestriate cortex of behaving rhesus monkey. J. Neurophysiol. *40*, 1392–1405.

Ponce, C.R., Lomber, S.G., and Born, R.T. (2008). Integrating motion and depth via parallel pathways. Nat. Neurosci. *11*, 216–223.

Prince, S.J., Pointon, A.D., Cumming, B.G., and Parker, A.J. (2002). Quantitative analysis of the responses of V1 neurons to horizontal disparity in dynamic random-dot stereograms. J. Neurophysiol. *87*, 191–208.

Qiu, F.T., and von der Heydt, R. (2005). Figure and ground in the visual cortex: v2 combines stereoscopic cues with gestalt rules. Neuron *47*, 155–166.

Ramsden, B.M., Hung, C.P., and Roe, A.W. (2001). Real and illusory contour processing in area V1 of the primate: a cortical balancing act. Cereb. Cortex *11*, 648–665.

Roe, A. (2003). Modular complexity of Area V2 in the macaque monkey. In The Primate Visual System, J.H. Kaas and C. Collins, eds. (New York, NY: CRC Press).

Roe, A.W., and Ts'o, D.Y. (1995). Visual topography in primate V2: multiple representation across functional stripes. J. Neurosci. *15*, 3689–3715.

Roe, A.W., Fritsches, K., and Pettigrew, J.D. (2005a). Optical imaging of functional organization of V1 and V2 in marmoset visual cortex. Anat. Rec. A Discov. Mol. Cell. Evol. Biol. *287*, 1213–1225.

Roe, A.W., Lu, H.D., and Hung, C.P. (2005b). Cortical processing of a brightness illusion. Proc. Natl. Acad. Sci. USA *102*, 3869–3874.

Sereno, M.E., Trinath, T., Augath, M., and Logothetis, N.K. (2002). Three-dimensional shape representation in monkey cortex. Neuron *33*, 635–652.

Shipp, S., and Zeki, S. (1985). Segregation of pathways leading from area V2 to areas V4 and V5 of macaque monkey visual cortex. Nature *315*, 322–325.

Shipp, S., and Zeki, S. (1989). The organization of connections between areas V5 and V2 in macaque monkey visual cortex. Eur. J. Neurosci. *1*, 333–354.

Shmuel, A., Korman, M., Sterkin, A., Harel, M., Ullman, S., Malach, R., and Grinvald, A. (2005). Retinotopic axis specificity and selective clustering of feedback projections from V2 to V1 in the owl monkey. J. Neurosci. *25*, 2117–2131.

Stepniewska, I., and Kaas, J.H. (1996). Topographic patterns of V2 cortical connections in macaque monkeys. J. Comp. Neurol. *371*, 129–152.

Swindale, N.V. (2004). How different feature spaces may be represented in cortical maps. Network *15*, 217–242.

Thomas, O.M., Cumming, B.G., and Parker, A.J. (2002). A specialization for relative disparity in V2. Nat. Neurosci. *5*, 472–478.

Tsao, D.Y., Vanduffel, W., Sasaki, Y., Fize, D., Knutsen, T.A., Mandeville, J.B., Wald, L.L., Dale, A.M., Rosen, B.R., Van Essen, D.C., et al. (2003). Stereopsis activates V3A and caudal intraparietal areas in macaques and humans. Neuron *39*, 555–568.

Ts'o, D.Y., Frostig, R.D., Lieke, E.E., and Grinvald, A. (1990). Functional organization of primate visual cortex revealed by high resolution optical imaging. Science *249*, 417–420.

Ts'o, D.Y., Roe, A.W., and Gilbert, C.D. (2001). A hierarchy of the functional organization for color, form and disparity in primate visual area V2. Vision Res. *41*, 1333–1349.

Wang, Y., Xiao, Y., and Felleman, D.J. (2006). V2 thin stripes contain spatially organized representations of achromatic luminance change. Cereb. Cortex *17*, 116–129.

Watanabe, M., Tanaka, H., Uka, T., and Fujita, I. (2002). Disparity-selective neurons in area V4 of macaque monkeys. J. Neurophysiol. *87*, 1960–1973.

Xiao, Y., Wang, Y., and Felleman, D.J. (2003). A spatially organized representation of colour in macaque cortical area V2. Nature *421*, 535–539.

Xu, X., Bosking, W., Sary, G., Stefansic, J., Shima, D., and Casagrande, V. (2004a). Functional organization of visual cortex in the owl monkey. J. Neurosci. *24*, 6237–6247.

Xu, X., Collins, C.E., Kaskan, P.M., Khaytin, I., Kaas, J.H., and Casagrande, V.A. (2004b). Optical imaging of visually evoked responses in prosimian primates reveals conserved features of the middle temporal visual area. Proc. Natl. Acad. Sci. USA *101*, 2566–2571.

Zeki, S., and Shipp, S. (1989). Modular connections between areas V2 and V4 of macaque monkey visual cortex. Eur. J. Neurosci. *1*, 494–506.